Electronic Supplementary Material (ESI) for Journal of Materials Chemistry B

Biophysical characterisation, antitumor activity and MOF encapsulation of a half-sandwich ruthenium (II) mitoxantronato system

S. Rojas, E. Quartapelle-Procopio, F. J. Carmona, M. A. Romero, J. A. R. Navarro* and E. Barea*

Departamento de Química Inorgánica, Universidad de Granada, Av. Fuentenueva S/N, 18071 Granada,

Spain. Fax: +34 958 248526; Tel:+34 958 248093; E-mail: JARN, jarn@ugr.es; EB, ebaream@ugr.es

SUPPORTING INFORMATION

Experimentals details

Materials and methods

^{1}H NMR experiments for the characterization of complex **1** and its interaction with cysteine and histidine, were performed in 0.75 mL MeOD solution with 5 mg of compound and 4 equivalents of the selected amino acid at 293 K. In the case of interaction with glutathione, the solvent was DMSO-d^6. ^{1}H NMR were recorded on a BRUKER ARX 400 (400 MHz) instrument (Centre of Scientific Instrumentation of the University of Granada). Elemental (C, H, N) analyses were obtained at a FISONS-CARLO ERBA EA 1008 analyzer (Centre of Scientific Instrumentation of the University of Granada). High resolution mass spectra with electrospray ionization (HRMS-ESI) were measured on a Waters Micromass LCT Premier mass spectrometer

The cyclovoltammetric study was performed at scan rates typically ranging 0.02 to 10 V s^{-1}, in HPLC-grade CH_3CN solutions at 2.5 10^{-5} M concentration deareated by N_2 bubbling, with tetrabutylammonium hexafluorophosphate $TBAPF_6$ (Fluka) 0.1 M as the supporting electrolyte, at 298 K. The ohmic drop was compensated by the positive feedback technique.[1] The experiments were carried out using an AUTOLAB PGSTAT potentiostat (EcoChemie, The Netherlands) run by a PC with GPES software. The working electrode was a glassy carbon (AMEL, ø =1.5 mm) cleaned by diamond powder (Aldrich, ø = 1 μm) on a wet cloth (STRUERS DP-NAP); the counter electrode was a Pt wire; the reference electrode was a saturated calomel electrode (SCE), having in our working medium a difference of –0.385 V vs. the $Fc^+|Fc$ couple (the intersolvental redox potential reference currently recommended by IUPAC[2]). The infrared spectra were recorded using a Perkin Elmer Spectrum GX IR spectrometer system with the spectral resolution of 2 cm^{-1}. The diffuse reflectance spectra were obtained in a VARIAN, mod. CARY-5E. N_2 adsorption isotherms were measured at 77 K on a Micromeritics Tristar 3000 volumetric instrument. Prior to measurement, powdered samples were activated by heating at 383 K for 7 h and outgassing to 10^{-4} bar. TEM analysis was done using a Philips CM-20 HR electron microscope operating at 200 keV with Energy Dispersive X-ray analysis (EDX). 2 mg of the material were redispersed by sonication (20 min) in 1 mL of EtOH. Carbon reinforced copper grids (200 meshs) were submerged into de suspension 50 times and then allowed to dry on air for at least 24 h.

*Synthesis of [(η^6-p-cymene)$_2$Ru$_2$mitoxantronato]Cl$_2$ (**1**).*

The reaction of mitoxantrone·HCl (1 mmol) with [Ru(*p*-cymene)Cl]$_2$Cl$_2$ (1 mmol) in ethanol (200 mL) at room temperature during 2 h gives rise to a dark green, limpid solution. The mixture is evaporated to dryness and **1** is extracted with CH_2Cl_2, precipitated by n-hexane addition and collected in moderate yield (48%) as a spectroscopically pure dark green solid.

Elemen. Anal. Calcd (%) for $[(C_{10}H_{14})_2Ru_2(C_{22}H_{26}N_4O_6)Cl_2](H_2O)_{3.5}$: C, 48.18; H, 5.87; N, 5.35. Found: C, 48.27; H, 6.12; N, 5.57.

^{1}HNMR (400 MHz, MeOD): δ (ppm), 7.53 (s, 2H, mito), 7.86 (s, 2H, mito), 5.67 (dd, 4H, Cy), 5.56 (d, 4H, Cy), 4.43 (dd, 2H, mito), 3.79 (m, 4H, mito), 3.64 (m, 2H, mito), 3.36 (m, 2H, mito), 2.93 (m, 2H, mito), 2.79 (m, 2H, Cy), 2.69 (m, 2H, mito), 2.20 (s, 6H, Cy), 2.05 (m, 2H, mito), 1.23 (m, 12H, Cy).

ESI mass spectra (MeOH) m/z + 948.1844 $[[(C_{10}H_{14})_2Ru_2(C_{22}H_{26}N_4O_6)Cl]^+$, 100%].

Biophysical characterisation of 1.

DNA binding studies

Calf-thymus (ct-DNA) was purchase from Sigma Aldrich. The ct-DNA was dissolved in water without further purification and kept frozen until the day of the experiment. The ct-DNA concentration (moles of bases per litre) was determined spectroscopically by using the molar extinction coefficient at the maximum of the long-wavelength absorbance (ct-DNA λ_{258} = 6600 cm^{-1} mol^{-1} dm^3). Concentrations of stock solutions of **1** and mitoxantrone were determined from accurately weighted samples of these materials.

Circular dichroism (CD) spectra were produced using a Jasco J-715 spectropolarimeter. UV-vis spectra were performed and visualized by ThermoSpectronic UV300 using 2 mL of ct-DNA (170 μM) in NaCl (20 mM) and sodium cacodylate buffer (1 mM). The previously described solutions were used to register UV-vis spectra with increasing quantities of **1** and mitoxantrone, keeping the ct-DNA concentration constant (ct-DNA/compound mixing ratios range from 200:1 to 3:1).

Ethidium bromide (EB) displacement by **1** and mioxantrone, was calculated by measuring the quenching of the EB fluorescence as it leaves the protection of the ct-DNA. A ct-DNA/salts/buffer solution with EB (ct-DNA/EB 4:5, 4 μM : 5 μM) was prepared. The emission spectrum was recorded as a function of **1** and mitoxantrone concentration by using a Variant mod. Cary Eclipse Luminescence spectrometer. The investigated compound concentration was slowly increased for ct-DNA/compound ratios from 200:1 to 1:1 keeping the ct-DNA and EB concentrations constant. Parameters for fluorescence spectra: λ_{em} = 600 nm, λ_{ex} = 540 nm, $slits_{em}$ = 15.0 nm, $slits_{ex}$ = 10.0 nm.

Cathepsin B enzymatic assay.

Crude bovine spleen cathepsin B was purchased from SigmaAldrich (C6286) and used without further purification. The colorimetric assay was performed in 20 mM sodium acetate and 1 mM EDTA (adjust to pH 5.1 with HCl 1M), using Na-CBZ-L-lysine *p*-nitrophenyl ester (CBZ = *N*-carbobenzoxy) as substrate. For the enzyme to be catalytically functional, the active site cysteine needs to be in the reduced form. Therefore, prior use, cathepsin B was prereduced with dithiothretiol (DTT) to ensure the majority of the enzyme is in a catalytically active form. Thus, cathepsine B was activated, before dilution, in the presence of an excess of DTT (1.2 eq) for 1h at 30 ºC.

IC_{50} determinations were performed in triplicate using a fixed enzyme concentration of 200 nM and a fixed substrate concentration of 100 μM. The enzyme and inhibitor were co-incubated at 30 ºC over a period of 24 h prior to the addition of substrate. Activity was measured over 4 min at 326 nm. Concentration of inhibitor is ranged between 0.3 and 50 μM (Figure S8).

Cathepsin D enzymatic assay

All the reagents were purchased from SigmaAldrich in the Cathepsin D Fluorimetric assay kit (CS0800) Crude bovine spleen cathepsin D (C3138) was used without further purification. The fluorimetric assay was performed in SigmaAldrich Assay Buffer 1x (A3855) with 2,5% Albumin Solution (A3980), using MCA-Gly-Lys-Pro-Ile-Leu-Phe-Phe-Arg-Leu-Lys(DNP)-D-Arg-NH2 trifloroacetate salt as substrate (1 mM solution, C4492). The final concentrations in the experiment were: cathepsin D ~ 5 nM, substrate

20 μM, 1 = 20 μM, mitoxantrone = 200 μM. The inhibition of the cathepsin D enzymatic activity by **1** (20 μM) is confirmed by the horizontal slope of the curve representing the hydrolysis of the substrate vs time. On the contrary, for mitoxantrone (200 μM), the same curve clearly shows the progressive hydrolysis of the substrate, that results in an increase of the fluorescence intensity vs time (Figure S9).

Biological assays

Cytotoxic studies were performed at the Pharmacological Activity Evaluation Unity, Industrial Pharmacy Institute, Faculty of Pharmacy, University of Santiago de Compostela, 15782 Santiago de Compostela, Spain. The tumor cell lines A2780, A2780cisR, were cultured at 37 ºC in RPMI 1640 medium (Gibco) supplemented with 10% FBS (Fetal Bovine Serum) and L-Glutamine 2 mM in an atmosphere of 95% of air and 5% CO2. Cell death was evaluated by using a system based on the tetrazolium compound MTT [3-(4,5-dimethyl-2-thiazolyl)-2,5-diphenyl-2*H*tetrazolium bromide], which is reduced by living cells to yield a soluble formazan product that can be detected colorimetrically. Cells were seeded in 96-well sterile plates at a density of 4000 cells/well in 100 μL of medium and were incubated 24 h. Complexes dissolved in DMSO were added to final concentrations ranging from 0 to 1.1 10^{-4} M in a volume of 100 μL/well. The final concentration of DMSO in cell culture was maintained in all cases at 1%. 96 h later, 10 μL of a freshly diluted MTT solution (2.5 mg/mL) was pipetted into each well and the plate was incubated at 37 °C in a humidified 5% CO2 atmosphere. After 5 h, the medium was removed and the obtained formazan product was dissolved in 100 μL of DMSO. The cell viability was evaluated by measurement of the absorbance at 595 nm. IC50 values (compound concentration that produces 50% of cell growth inhibition) were calculated from curves constructed by plotting cell survival (%) versus drug concentration (μM). All experiments were made in triplicate.

Drug encapsulation strategy

Synthesis of $[Fe^{III}_3F(H_2O)_2O(C_6H_3(CO_2)_3)_2 \cdot nH2O\ (n \sim 14.5)]$ *(**MIL100(Fe)**)*

MIL100(Fe) was prepared form hydrothermal reaction of trimesic acid with metallic iron, HF, nitric acid and H_2O at 433 K for 8 h as previously reported in literature.[3] In a typical synthesis, the composition of reaction mixture was 55.84 mg (1.0 mmol) of Fe

(0): 138.7 mg (0.67 mmol) of 1,3,5-BTC = benzene tricarboxylic or trimesic acid: 35 µl (2.0 mmol) of HF: 50 µl (0.6 mmol) HNO_3: 5 ml (277 mmol) of H_2O.

The as synthesized **MIL100(Fe)** was further purified by a two-step process using double solvent extraction with hot water and ethanol: 200 mg of the solid were suspended in 100 ml of deionized water at 343 K for 3 h and afterwards in 100 ml of ethanol at 338 K for 3 h.

Synthesis of ***MIL100(Fe)@Ru(H$_2$O)$_3$Cl$_3$***

Prior to the loading of the ruthenium compounds into **MIL100(Fe)**, the as synthesized solid **MIL100(Fe)** was heated at 383 K for 7 h and outgassed to 10^{-4} bar. Under these conditions, the complete removal of the water guest molecules was achieved in order to obtain empty pores ready for adsorption of other guest molecules.

210 mg of $Ru(H_2O)_3Cl_3$ (1.01 mmol) were dissolved in 20 ml of acetone. Then 200 mg of **MIL100(Fe)** (0.324 mmol) were added, and the mixture was grinded in order to speed up the solvent evaporation to increase the concentration of the solution (until all the solvent is gone). Finally, the solid product was whashed with acetone (10 ml x 2) to eliminate the excess of free $Ru(H_2O)_3Cl_3$.

Elemen. Anal. Calcd (%) for $Fe_3OF(C_9H_3O_6)_2(Ru(H_2O)_3Cl_3)_2(H_2O)_5(C_3H_6O)$ (**MIL100(Fe)@Ru(H$_2$O)$_3$Cl$_3$**): C, 20.15; H, 2.42. Found: C, 20.01; H, 2.23.

Synthesis of ***MIL100(Fe)@[Ru(p-cymene)Cl]$_2$Cl$_2$***

700 mg of MIL100(Fe)@$Ru(H_2O)_3Cl_3$ (0.68 mmol) and 1.1 ml of α-terpinene (6.8 mmol) were refluxed in ethanol (80 ml) for 24h. Then the solid was filtered and washed with EtOH (10 ml x 2).

Elemen. Anal. Calcd (%) for $Fe_3OF(C_9H_3O_6)_2(C_{20}H_{28}Cl_4Ru_2)_{0.5}(H_2O)_5(Ru(H_2O)_3Cl_3)$ (**MIL100(Fe)@[Ru(*p*-cymene)Cl]$_2$Cl$_2$**): C, 26.39; H, 2.85. Found: C, 26.36; H, 2.92.

Synthesis of ***MIL100(Fe)@1***

200 mg of MIL100(Fe)@[Ru(*p*-cymene)Cl]$_2$Cl$_2$ (0.16 mmol) and 72 mg of mitoxantrone·HCl (0.16 mmol) were heated with 50 ml of ethanol at 313 K during 24 h. Then, the solid was filtered and washed with EtOH (10 ml x 2).

Elemen. Anal. Calcd (%) for $Fe_3OF(C_9H_3O_6)_2(C_{42}H_{54}N_4O_6Ru_2)_{0.4}(C_{20}H_{28}Cl_4Ru_2)_{0.1}(H_2O)_{11}(Ru(H_2O)_3Cl_3)$ (**MIL100(Fe)@1**): C, 29.41; N, 1.49; H, 3.92. Found: C, 28.73; N, 1.52; H, 2.91.

^{1}H NMR spectra

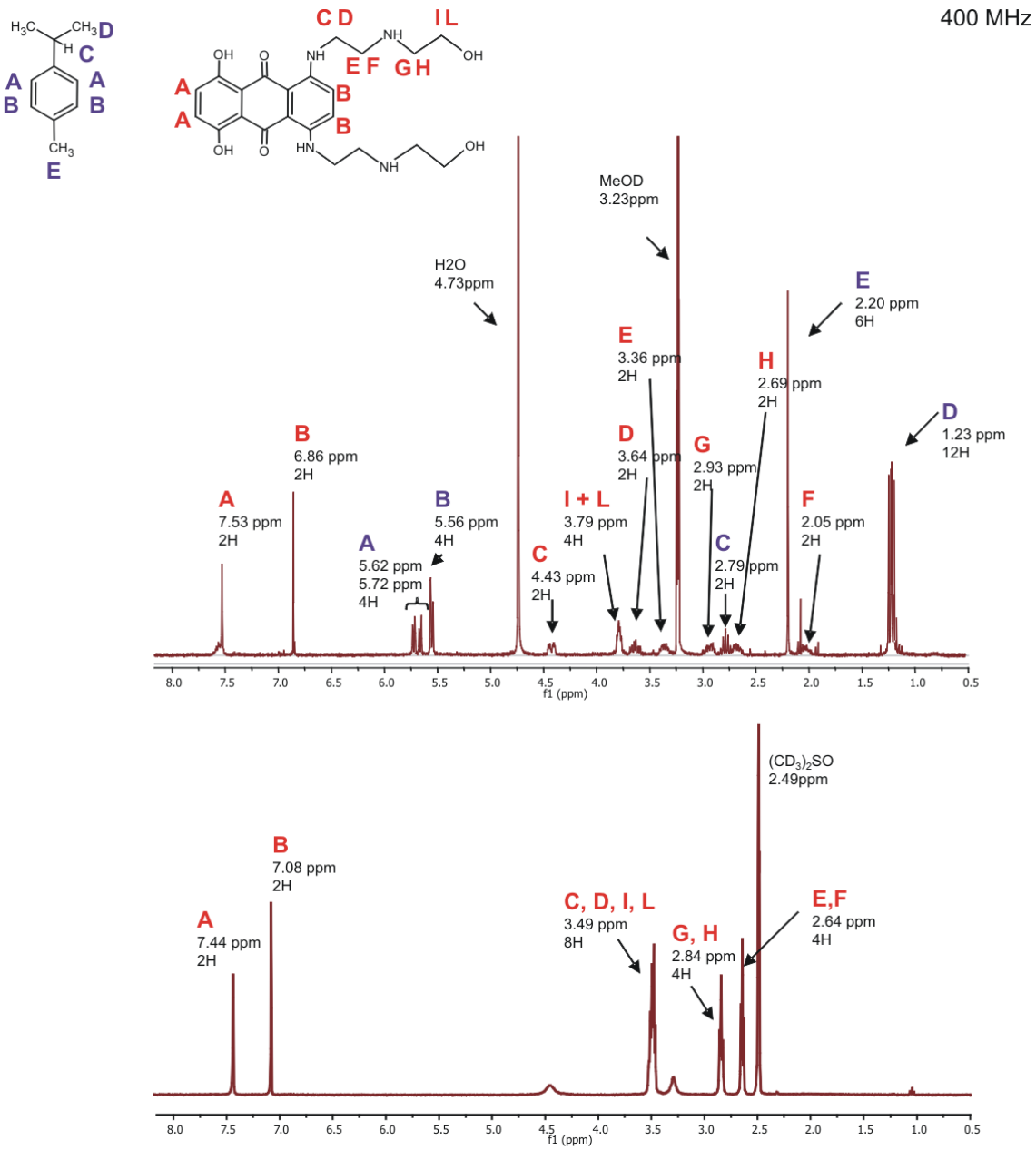

Figure S1. ^{1}H RMN spectra of **1** (top) **(**MeOD, 400 MHz) and free mitoxantrone (bottom) (DMSO, 400 MHz).

ESI-MS

The ESI-MS spectrum of **1** shows the highest intensity peak at m/Z = 948.1844 that correspond to the complex $[(p\text{-}Cy)_2Ru_2mitoxantronate]Cl^+$.

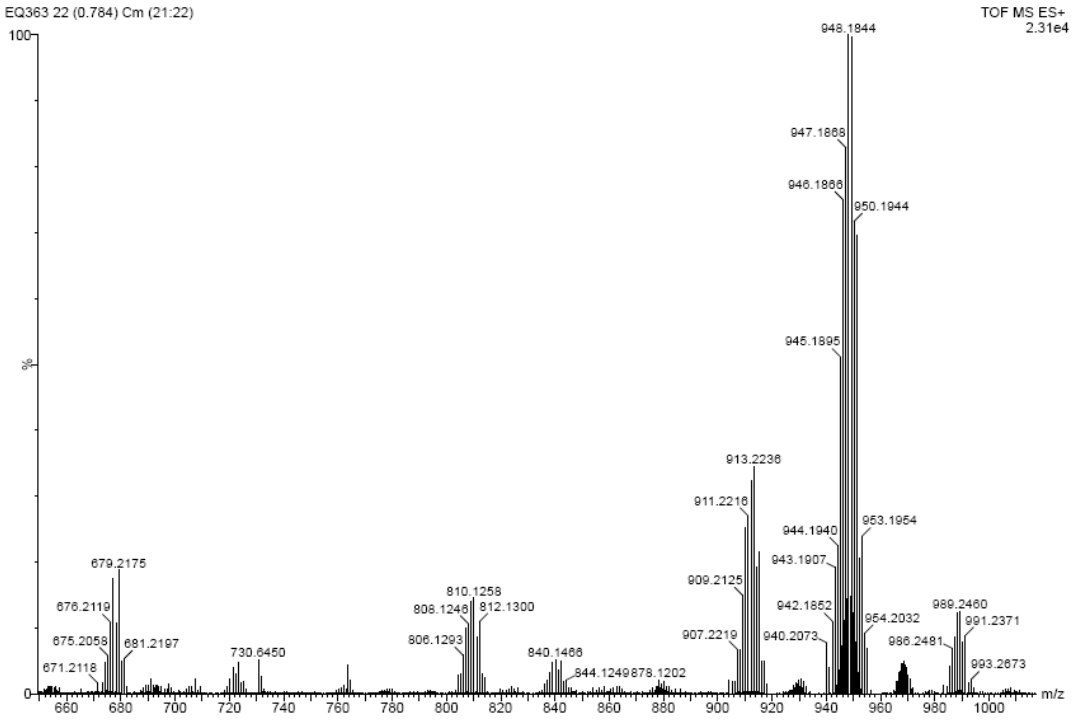

Figure S2. ESI MS+ spectra of **1** in MeOH.

Cyclic voltammetry

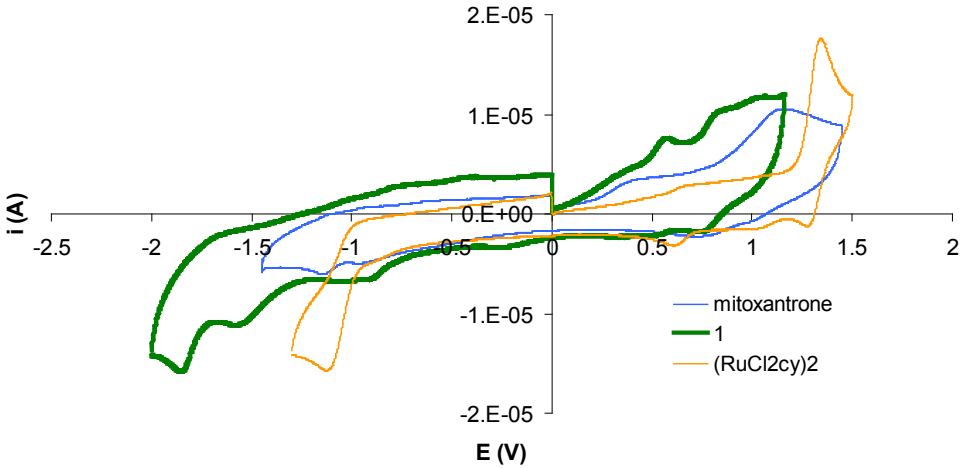

Figure S3. Superposition of the cyclic voltammogram (c-a) for **1**, mitoxantrone and $[Ru(p\text{-}cy)Cl]_2Cl_2$.

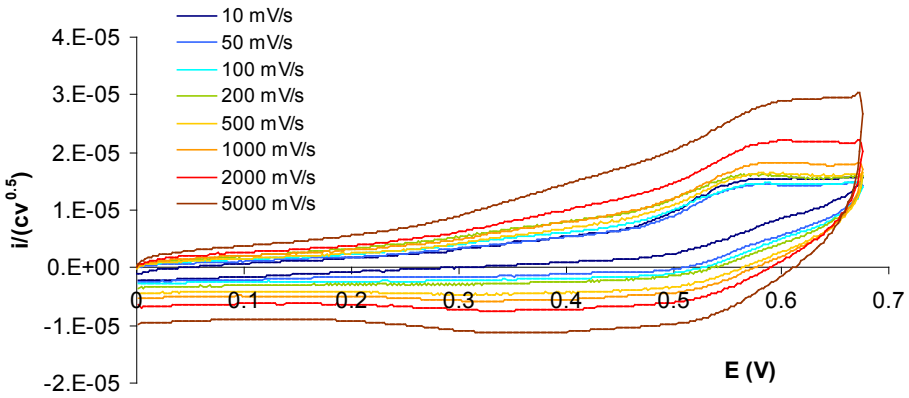

Figure S4. Effect of the increasing scan rate on first anodic peak of **1**.

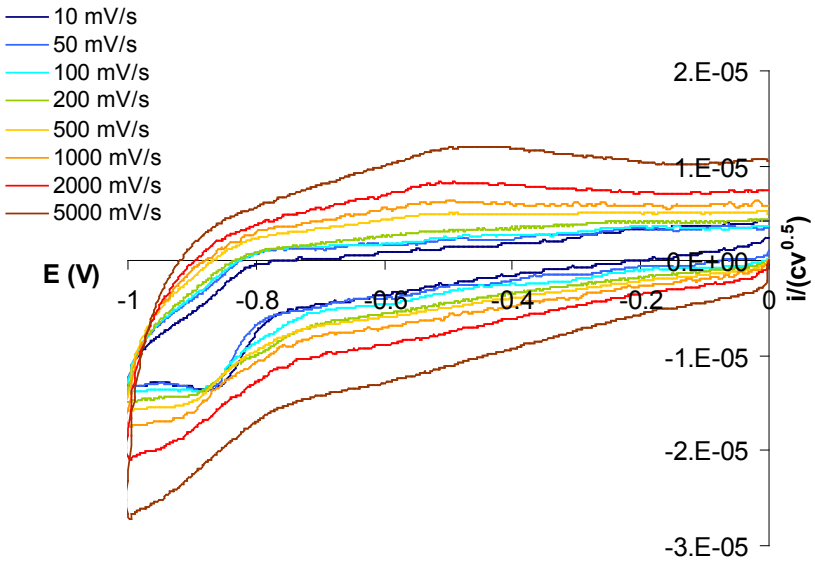

Figure S5. Effect of the increasing scan rate on the first cathodic peak of **1**.

Circular dichroism

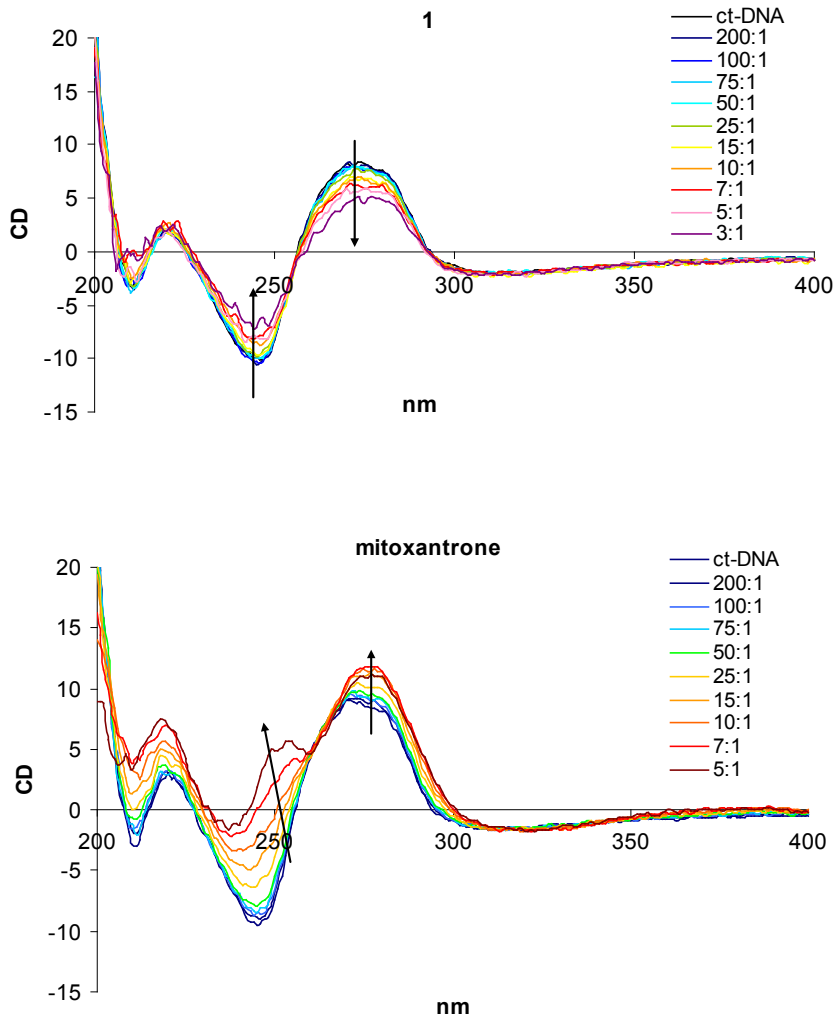

Figure S6. CD spectra of the titration of ct-DNA (170 μM in a 1 mM sodium cacodylate buffer and 2 mM NaCl) with **1** (top) and mitoxantrone (bottom), in 200:1 to 3:1 ratio.

Reactivity with S- and N-donor amino acids

a)

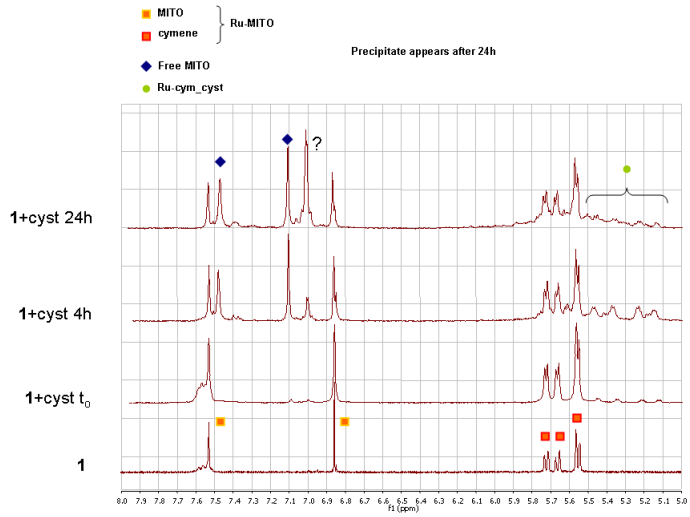

b)

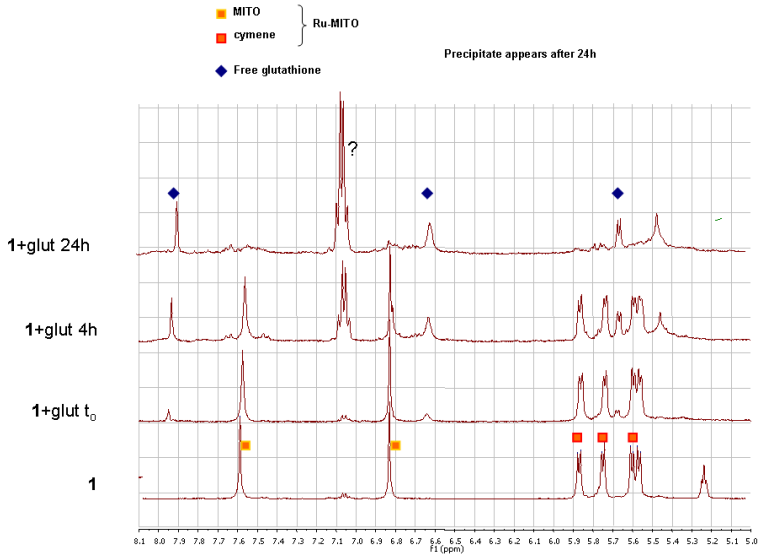

c)

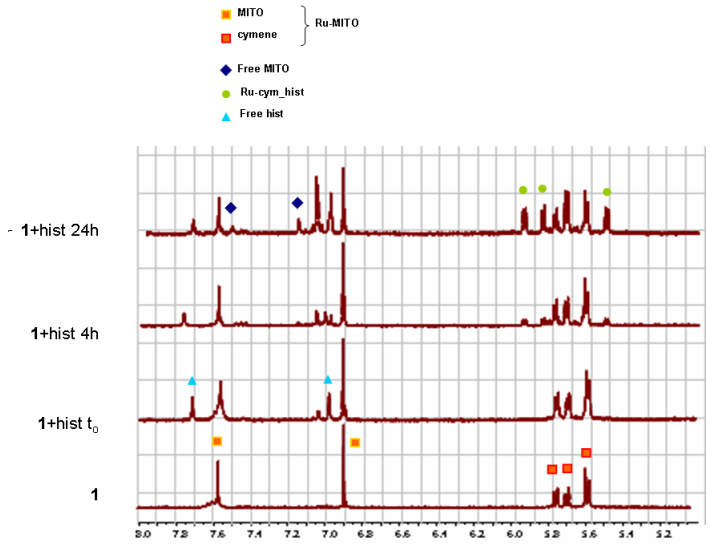

Figure S7. ^{1}H NMR spectra, over 24 h, of the interaction of **1** with relevant S-donor biomolecules (cysteine (a) and glutathione (b)).

Cathepsin B enzymatic assay

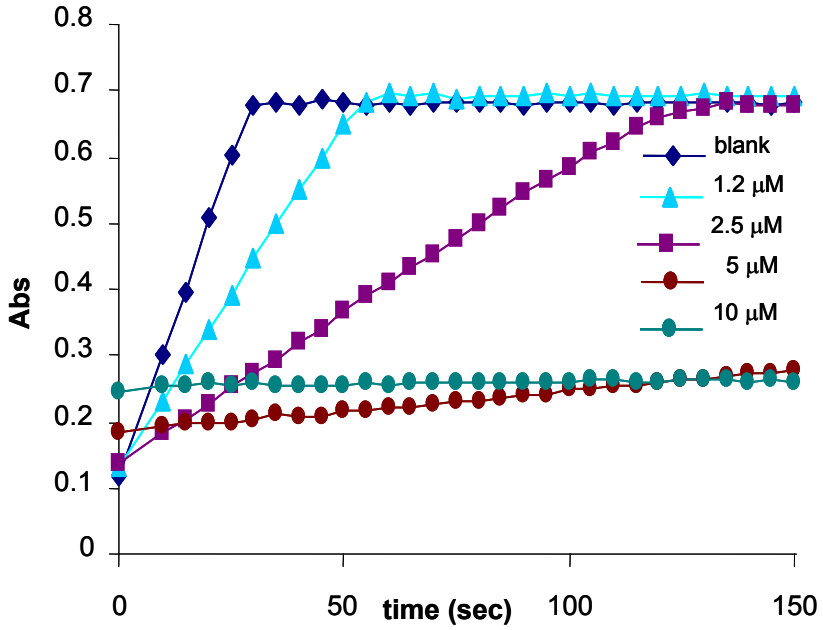

Figure S8. Concentration dependant cathepsin B inhibition assays by **1**.

Cathepsin D enzymatic assay

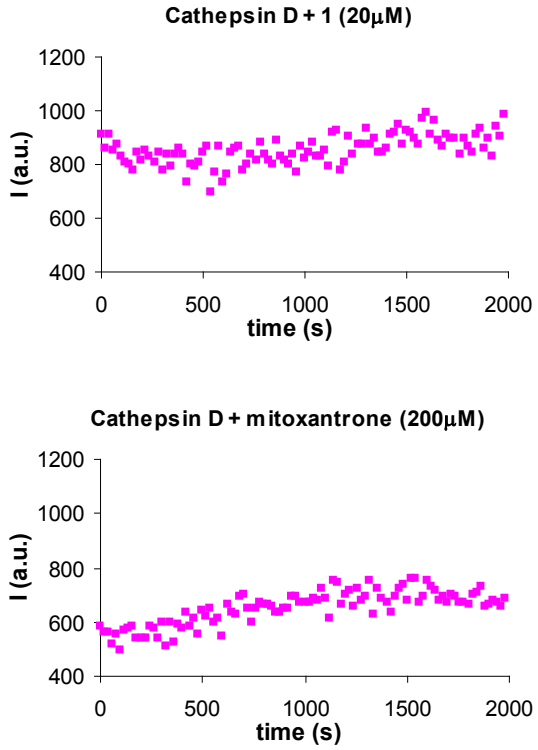

Figure S9. Cathepsin D enzymatic assay with **1** (20 μM) (top) and mitoxantrone (200 μM) (bottom).

Encapsulation of 1 into MIL100(Fe)

IR spectra

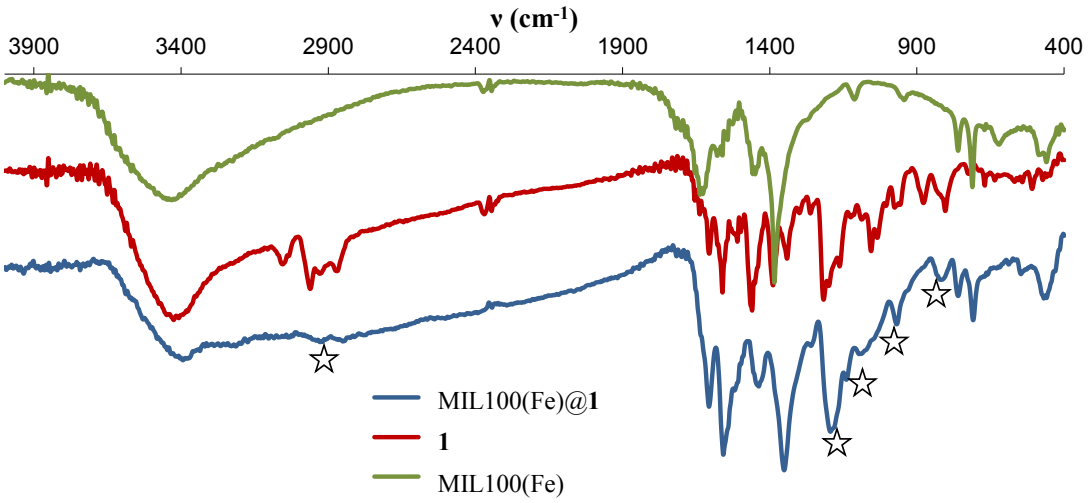

Figure S10. IR spectra of **1**, **MIL100(Fe)** and **MIL100(Fe)@1** samples. Stars denote the characteristic features of **1** in the mixed system **MIL100(Fe)@1**.

Diffuse reflectance spectra

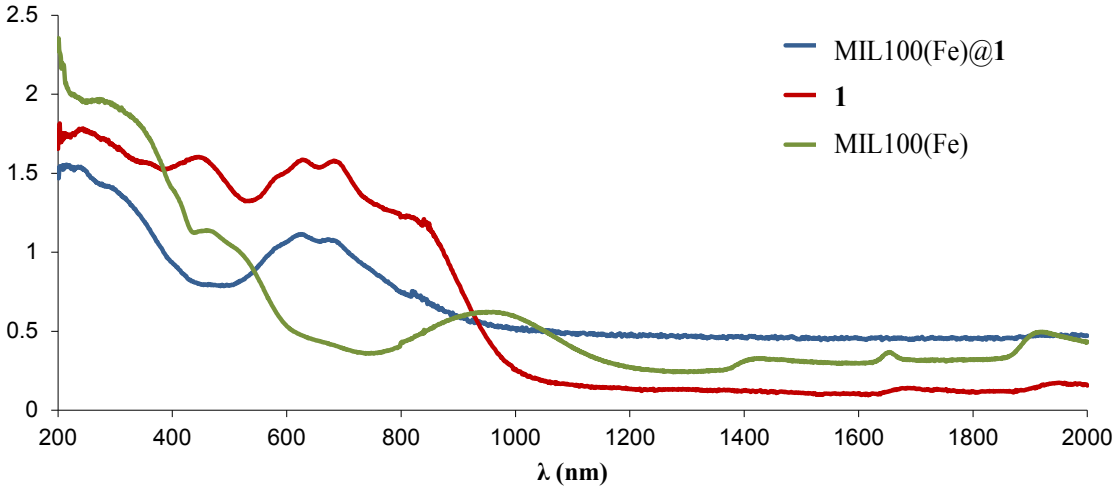

Figure S11. Diffuse reflectance spectra of **1**, **MIL100(Fe)** and **MIL100(Fe)@1**.

N_2 adsorption isotherms

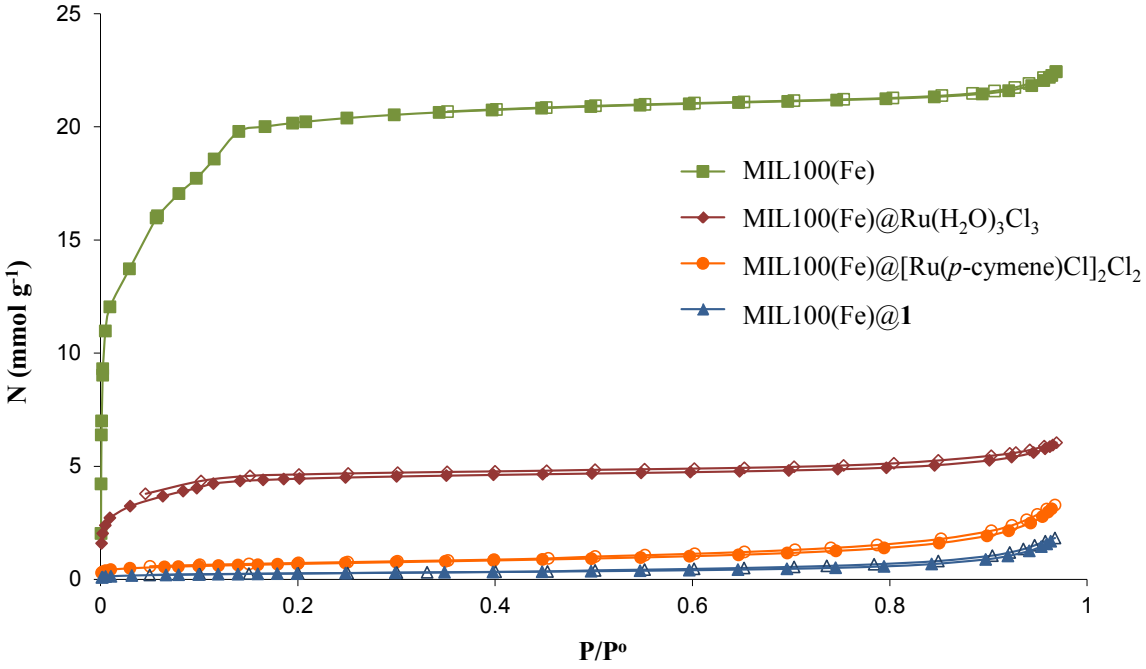

Figure S12. N_2 adsorption isotherms at 77 K for activated **MIL100(Fe)** (green squares), **MIL100(Fe)@Ru(H_2O)$_3Cl_3$** (red diamonds), **MIL100(Fe)@[Ru(*p*-cymene)Cl]$_2Cl_2$** (orange circles) and **MIL100(Fe)@1** (blue triangles). Empty symbols denote desorption.

TEM

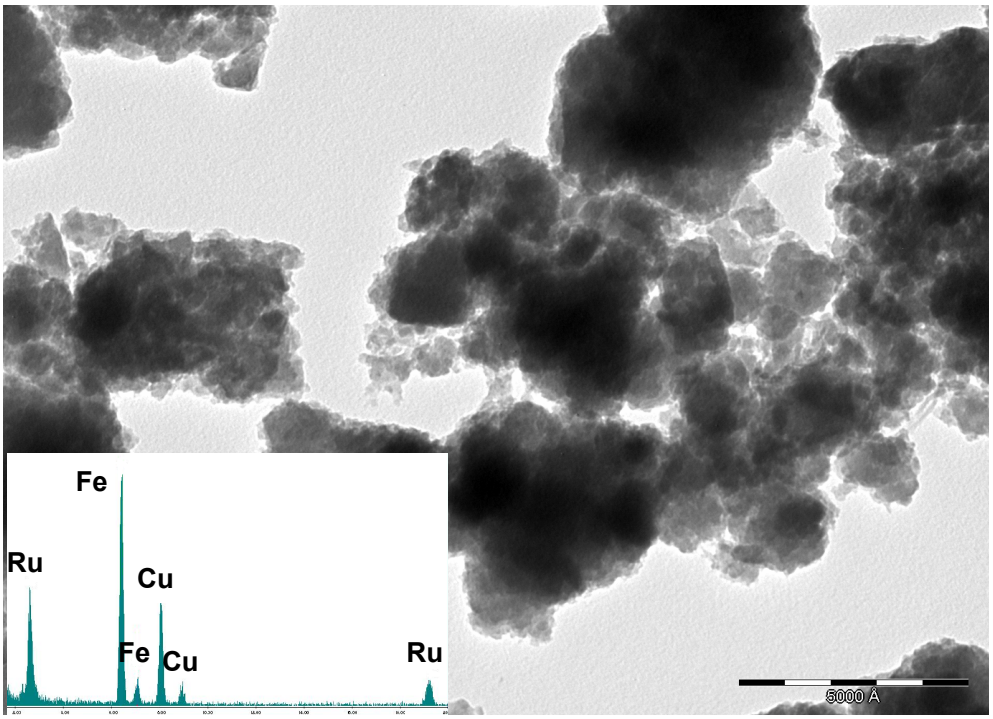

Figure S13. TEM images of **MIL100(Fe)@1** (top). Chemical characterization of **MIL100(Fe)@1** from energy-dispersive X-ray spectroscopy data (bottom).

[1] A. J. Bard, L. R. Faulkner, in Electrochemical Methods: Fundamentals and Applications, Wiley, New York 2002, pp. 648.

[2] G. Gritzner, J. Kuta, *Pure Appl. Chem*. 1984, **56**, 461-466.

[3] Y. Seo, J. Yoon, J. Lee, U. Lee, Y. Hwang, C. Jun, P. Horcajada, C. Serre, J. Chang, *Microporous and Mesoporous Materials,* 2012, **157,** 137–145.